

Fission Cross Section of ^{238}Pu

M. G. Silbert

Los Alamos Scientific Laboratory, University of California

Los Alamos, New Mexico, U.S.A.

and

A. Moat

Atomic Weapons Research Establishment

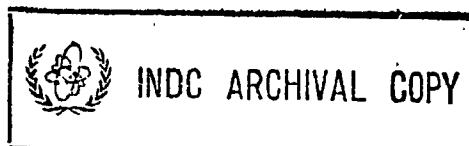
Aldermaston, England

and

T. E. Young

Aerojet Nuclear Corporation, National Reactor Testing Station

Idaho Falls, Idaho, U.S.A.



Fission Cross Section of ^{238}Pu †

M. G. Silbert

Los Alamos Scientific Laboratory, University of California

Los Alamos, New Mexico

and

A. Moat

Atomic Weapons Research Establishment

Aldermaston, England

and

T. E. Young

Aerojet Nuclear Corporation, National Reactor Testing Station

Idaho Falls, Idaho

ABSTRACT

The neutron-induced fission cross section of ^{238}Pu was measured from 18 eV to 3 MeV. The nuclear explosion Persimmon provided an intense, single-pulse neutron source spanning an energy range of more than five decades. Neutrons from this underground source were sorted by time of flight over a 300-m vertical path and interacted with a ^{238}Pu sample and with flux monitors at ground level. Fission cross-section areas are reported for 49 resonances below 500 eV. A number of previously unobserved resonances are reported, yielding an average level spacing of 9.5 ± 1 eV. There is strong evidence for intermediate structure in the fission cross section with an average spacing of about 1 keV.

I. INTRODUCTION

The neutron-induced fission cross section of ^{238}Pu is of interest in understanding the fission process and in tracing the systematic properties of heavy nuclei. Plutonium-238 shares the property common to the lightest uranium and plutonium even-target isotopes of exhibiting substantial sub-threshold fission. Furthermore, the fission cross section demonstrates the intermediate structure that has been attributed to the interaction between normal compound nucleus energy levels and the much more widely spaced levels in a secondary potential well in a double-peaked fission barrier.

In addition to its interest in the study of the fission process, ^{238}Pu has applications as one of the most favorable isotopic heat sources. In processing large quantities of the material it is useful to have a knowledge of its fission cross section so that problems of nuclear criticality may be assessed.

This paper describes a measurement of the neutron-induced fission cross section of ^{238}Pu between 18 eV and 3 MeV. Substantial resonance fission was observed, and the level of the subthreshold cross section was high enough so that it increased by only a factor of three over the threshold region as the neutron energy increased from 0.1 MeV to the plateau between 1 and 3 MeV.

Among the nuclei in this region of the periodic table are many whose inherent alpha-particle and spontaneous-fission decay presents experimental problems in fission cross-section measurements with accelerator neutron sources. The alpha-particle and spontaneous-fission half lives of ^{238}Pu are 87.5 yr and 5×10^{10} yr, respectively, so that special detection methods have frequently had to be employed in laboratory measurements to cope with the intense sample activities. One advantageous feature of the nuclear

explosion source is its extremely high neutron intensity. At a flight path of 300 m the inherent radioactivity of ^{238}Pu was negligible compared to the neutron-induced reaction rate.

A number of measurements of the $^{238}\text{Pu}(n,f)$ cross section have been reported. They divide into two categories: (1) measurements with slow neutrons from time-of-flight linac experiments, and (2) measurements with fast monoenergetic neutrons from electrostatic accelerators. In the resonance region, Stubbins *et al.*¹ reported resonance fission from 2 to 300 eV while Gerasimov² measured the cross section from 0.02 to 400 eV.

In the fast neutron region, an early measurement was reported by Butler and Sjoblom³ between 0.14 and 1.75 MeV. More recent experiments have been made by Vorotnikov *et al.*⁴ (50 to 1400 keV), Barton and Koontz⁵ (1.0, 1.5, 3.0, 14.9 MeV), Ermagambetov and Smirenkin⁶ (0.5 to 5.6 MeV, 13 to 16.9 MeV), Ermagambetov and Smirenkin⁷ (2.7 to 1000 keV), and Fomushkin and Gutnikova⁸ (0.44 to 3.6 MeV).

Two measurements of the $^{238}\text{Pu}(n,f)$ cross section have been made by the time-of-flight technique with nuclear explosion neutron sources. The first of these, on the Persimmon event, is reported here in final form and was presented previously in a preliminary report.⁹ The second, on the Pommard event, was reported by Drake *et al.*¹⁰ The measurements with nuclear explosion sources have the advantage of covering a very wide neutron energy range, greater than five decades, and allow study with good resolution of the region from 1 to 100 keV that exhibits intermediate structure. Below 500 eV, the experimental resolution was sufficient to resolve essentially all the observed resonances, and the sensitivity to small cross sections was sufficient to detect previously unreported small resonances, even below 100 eV where Stubbins *et al.*¹ and Gerasimov² were able to resolve the larger resonances readily.

In addition to the fission cross-section measurements listed above, the total cross section of ^{238}Pu has been reported by Young *et al.*¹¹ from 0.008 to 6500 eV. In a subsequent paper we will describe a measurement of the ^{238}Pu radiative neutron capture cross section, also performed on the Persimmon event, and an analysis of the neutron and fission widths of some 50 resonances below 500 eV, obtained from a combination of the fission and capture resonance areas.

II. EXPERIMENTAL METHOD

*Note to editor:
third subheading* → A. General. The present work utilized the neutron time-of-flight method, with the intense single burst of neutrons released by the underground nuclear explosion Persimmon as the source. A general description of this method of using such neutrons in cross-section measurements is given in Ref. 12, while Refs. 13 through 16 provide further information. Reference 9 is a preliminary report of the present measurement.

Persimmon was a nuclear explosion detonated at a depth of 300 m in February 1967. An evacuated vertical pipe allowed a well-collimated, 1.9-cm diameter beam of neutrons to enter the experimental apparatus at ground level. The neutron beam then passed through a series of thin target foils in a large vacuum chamber. The slowest neutrons observed traversed the 300-m flight path in about 5 msec and had an energy of 17 eV.

Detection of fission fragments from the reaction $^{238}\text{Pu}(n,f)$ provided a signal proportional to the cross section being measured. A blank backing foil determined the background. The neutron flux was monitored by the reactions $^{235}\text{U}(n,f)$, $^6\text{Li}(n,\alpha)$, and $^3\text{He}(n,p)$.

B. Detectors, recording. The reaction products from each target foil were detected by semiconductor particle detectors positioned close to the foils but outside the neutron beam. Each foil was at 45° to the neutron beam. The detectors, each subtending a solid angle of about 0.1 sr at its foil center, were oriented at 55° , 80° , or 90° to the neutron beam. They were positioned so that each detector was at 45° to its target foil; particle energy loss in the foil would then be the same for the three angles of observation, except for small effects of finite detector and beam size.

The semiconductor detectors viewing the ^{238}Pu sample were protected from alpha-particle bombardment by a camera shutter between the sample and the detectors that opened one second before explosion zero time and closed at two seconds after zero time. Radiation damage to the detectors by alpha particles and fission fragments during the time the shutter was open was negligible. The detector current due to alphas, while the shutter was open, was negligible compared to the neutron-induced fission fragment signal.

Detector solid angles were measured before the experiment by alpha-particle counting an absolutely calibrated ^{239}Pu deposit inserted in place of the target foils, with a size and elliptical shape to simulate the intersection area of the circular neutron beam and the 45° targets.

Since the reaction rates were in general too high to allow observation of individual particles, the detectors were operated as current generators. The output current at any point in time was proportional to the product of the neutron flux and the target cross section for the neutron energy corresponding to that flight time.

Detector currents were amplified logarithmically to reduce the dynamic range necessary for recording, and were then displayed on oscilloscopes for photographic recording. Since it was desired to achieve time resolution of less than 1 μ sec for a duration of 5 msec, the oscilloscope traces were recorded by moving-film cameras in a streak mode. The amplified detector signals were applied to one set of the oscilloscope deflection plates and the time base was provided by film motion at 90° to the direction of oscilloscope deflection. Each such photographic record also contained a base-line reference trace and a set of precision time marks. One or more sets of amplifier calibration signals were recorded several msec after the lowest energy neutrons had been detected.

In this method of current recording, detector current was proportional to the product of the number of reaction particles entering the active region per unit time and the average energy per particle converted to electron-hole pairs in the silicon. The silicon depletion regions were deep enough so that all the particles of interest (fission fragments from ^{238}Pu and ^{235}U , protons from ^3He , tritons and alpha particles from ^6Li) were stopped within them. Particle energy deposited in the detectors was calculated as described in Ref. 17, taking into account initial particle energy from the nuclear reaction, losses in the target material and detector front dead layer, and, for fission fragments, the discrepancy between fragment energy and observed current termed the fission fragment defect.

C. Neutron flux. Systematic errors are minimized when the flux is determined from a known fission cross section, since comparison is then made between two fission signals. This procedure was possible above 10^3 eV, where the ^{235}U fission cross section was used as the standard. Above 5×10^5 eV the ^{235}U fission fragment angular distribution departs from isotropy; for those energies, values of $4\pi(d\sigma/d\Omega)$ appropriate to the 55° and 90° observation angles were used.

At energies below 10^3 eV the resonance structure of ^{235}U fission precludes its use as a direct standard, so the smoothly varying $^3\text{He}(n,p)^{18}$ and $^6\text{Li}(n,\alpha)$ reactions were used to determine the flux in the energy regions 10^1 to 10^2 eV and 10^2 to 10^3 eV respectively. However, as a check on the consistency of these standards with $^{235}\text{U}(n,f)$, they have been used to generate the $^{235}\text{U}(n,f)$ cross section from the ^{235}U signals. Integrals of that cross section are compared in Table I with integrals of the cross section given by de Saussure.¹⁹

The standards upon which the flux was based are summarized as follows:

Below 10^2 eV	$^3\text{He}(n,p)$, assumed $1/v$ dependent from 5327 barns at 0.0253 eV.
10^2 to 10^3 eV	$^6\text{Li}(n,\alpha)$, assumed $1/v$ dependent from 940.8 barns at 0.0253 eV.
10^3 to 10^4 eV	$^{235}\text{U}(n,f)$, using cross section of de Saussure <u>et al.</u> ¹⁹
Above 10^4 eV	$^{235}\text{U}(n,f)$, using the evaluation of Davey, ²⁰ listed in Table II.

The neutron flux as a function of neutron energy is illustrated in Fig. 1 of Ref. 9.

The neutron source was composite because a neutron moderator was placed in the beam pipe just above the nuclear explosive. An explosion source alone would provide neutrons only down to about 10^3 eV. The polyethylene moderator, sandwiched between lead sheets to reduce its temperature and bulk motion, served as a secondary source of neutrons with energies down to 17 eV.

D. Background. The background signal, measured by detectors viewing a bare platinum foil backing, exhibited two components: (1) resonance structure corresponding to neutron capture in platinum, below 10^4 eV, and (2) a smoothly varying signal that increased with neutron energy, above 10^4 eV. In the region below 10^4 eV, both the ^{238}Pu signal and the background signal had pronounced resonance structure, with the larger platinum peaks being comparable in size with the smaller ^{238}Pu peaks. Above 10^4 eV, the signal-to-background ratio was ≥ 10 , so that background subtraction introduced little error. Several of the prominent platinum resonances, notably the doublet at 66.9/67.5 eV, could be readily observed both in the background and in the ^{238}Pu signals and served to determine the normalization factor for background subtraction.

In addition to their response to fission fragments, the fission detectors were sensitive to a certain degree to gamma rays and thus to neutron capture in the samples. Measurements with ^{238}U and ^{244}Pu targets, as well as those with the platinum backings, determined that the detector signal corresponding to a capture event was about 1.5×10^{-3} the signal corresponding to a fission event. For ^{238}Pu , the fission-to-capture ratio

is large enough that this effect was negligible compared to other uncertainties, and no corrections have been applied. Fission detector response to fission gamma rays and fission neutrons was negligible compared to the response to fission fragments.

Another effect, beam fuzz due to imperfect collimation and to neutron scattering in the chamber windows and in the samples, related to neutrons outside the beam having essentially the same time-energy relation as those in the beam itself. Several measurements were made of neutrons outside the beam. One such measurement provided a sheet of sulfur-loaded plastic with a central hole through which the beam passed. Neutrons outside the main beam with energies above about 2 MeV activated the sheet by the $^{32}\text{S}(n,p)$ reaction. Subsequent counting of the ^{32}P activity in slices of the sheet, with a low-background beta counter, provided a measure of the beam fuzz. A second determination was made by covering a standard detector with a cap having a ^{235}U deposit on its inside surface. Comparison of the size of ^{235}U resonances in the signal from the capped detector and a signal from a regular detector viewing the ^{235}U sample in the beam provided another measure of beam fuzz, in this case for resonance-energy neutrons. Both of these measurements of beam fuzz showed that at normal detector distances of 2 to 5 cm from the center of the neutron beam, the neutron flux (in neut/cm²-sec) was a few times 10^{-5} of that in the beam.

Still another background effect to be considered is the possible presence of neutrons at the samples with an incorrect time-energy relationship. Such neutrons might have been produced by a number of

mechanisms, including back-scatter of the neutron beam. Perhaps the best test for such neutrons was observation of peak-to-valley ratios for neutron resonances, because wrong-energy neutrons tended to fill in the valleys. In our experimental arrangement this effect was small since peak-to-valley ratios were excellent, most notably in the ^{239}Pu cross section measured on the Petrel event.¹³

E. Energy scale. The neutron energy scale was derived from the standard equation $E_n = 5226.7 (D/\Delta t)^2$, with E_n in electron volts, the flight path D in meters, and the flight time Δt in microseconds.

Time of flight was determined from timing marks produced on the film records by a precision oscillator simultaneously with data recording. The intense, short-duration peak produced in each signal by the gamma ray flash occurring at explosion time provided a zero for the time scale for those neutrons directly from the explosion. Neutrons from the polyethylene moderator were delayed and spread out in time of emission by the diffusion and slowing-down process, with an effective shift in zero time.

The time-mark generator was rated at an accuracy of ± 1.5 parts per 10^5 , which yields an uncertainty of ± 0.075 μsec at 5 msec flight time. The uncertainty in the measurement of zero time by observation of the gamma flash is estimated to be ± 0.2 μsec . An indication of the reliability of the energy scale for high energy (direct from the explosion) neutrons was given by observation of a sharp dip in the neutron flux due to a prominent resonance in ^{208}Pb . (Lead, in the neutron beam above and below the polyethylene moderator, reduced moderator heating and motion.) This

measurement gave a value of 78.3 ± 0.4 keV for the resonance, which can be compared to 77 keV measured by Gibbons and Macklin²² and 80 keV measured by Bilpuch et al.²³

The flight path from the device center and from the moderator to the targets was known from direct mechanical measurements of the lengths of the beam pipe and associated structural members. The uncertainty in the original 300-m flight path is estimated to be ± 0.1 m, or 0.033%, so that the corresponding uncertainty in E_n is 0.07%. Since the moderator could move upward in response to the explosion under it, the flight path at the time of peak moderator neutron emission could have been less than the original distance. Both the moderator position and the time of emission of moderated neutrons, assumed for simplicity to have been the same for all neutrons with energies below 10^3 eV, were determined from the data by observation of resonances in ^{235}U , Pt, and ^{238}Pu whose energies were assumed to be known. This analysis yielded a moderator position 0.5 m above the device center, consistent with its original position, and a delay of 2 μsec to the peak of neutron emission. The energy scale below 10^3 eV was therefore based on the assumed resonance energies from BNL-325²⁴ for ^{235}U and Pt, and from Young et al.¹¹ for ^{238}Pu .

The resultant energy scale has an arbitrary discontinuity at 10^3 eV, with an overlap of 2.4 eV at this point.

F. Energy resolution. The factors influencing the experimental neutron energy resolution include (1) the flight path, (2) the source time width, (3) the source size, (4) the experimental resolving time, and (5) the Doppler width.¹⁴ In this experiment, two separate neutron

sources were involved: the explosion itself with a source time width of less than 0.1 μ sec and the polyethylene moderator with a source time width of 6 μ sec (FWHM). The neutron pulse from the moderator, as observed in isolated, inherently narrow resonances, exhibited a skewed time distribution with a rapid rise and a slow decay. The electronics and recording system had a time resolution limitation of 0.2 to 0.3 μ sec. These resolving times and flight paths imply a resolution of 20 nsec/m in the resonance region below 10^3 eV and 0.7 nsec/m for higher energy neutrons.

G. ^{233}Pu target foil. The sample deposit was PuO_2 evaporated in a 4-cm diameter circle onto a backing of 0.00063-cm (0.00025-inch) thick platinum soldered to a support ring. The total weight of ^{238}Pu was determined by low-geometry alpha-particle counting to be 5.14 ± 0.15 mg, assuming a half life of 87.5 years. Detailed survey of the distribution of the deposit showed a concentration of material toward the center so that the average density of ^{238}Pu at the position of the 1.9-cm diameter neutron beam was $441 \mu\text{g}/\text{cm}^2$, rather than the $403 \mu\text{g}/\text{cm}^2$ that would correspond to a uniform deposit.

The sample had an isotopic composition of ^{233}Pu - 99.47%, ^{239}Pu - 0.49%, ^{240}Pu - 0.04%, and ^{241}Pu - < 0.01%, as determined by mass spectroscopy. Based on the age of the sample from chemical separation to the time of the experiment, the amount of ^{234}U daughter was 0.2%.

III. DATA

Data recording, processing, and reduction to cross sections were done independently by groups from IASL and from AWRE. The ^{238}Pu fission cross sections reported here were generated by four semiconductor detectors, one pair at 55° and 80° (IASL) and the other pair at 55° and 90° (AWRE). The signal from each IASL detector was recorded by two separate cameras, a high-resolution (0.2 μsec) drum camera and a low-resolution (1.0 μsec) streak camera. The signal from each AWRE detector was recorded by a high-resolution (0.3 μsec) disk camera that covered the entire energy range.

The common features of the two sets of data, obtained simultaneously on the Persimmon event, are the flux and background measurements and the fissile deposit. Some of the major experimental differences are listed in Table III.

For the IASL data, the time channels chosen were 1.0 μsec up to 10^5 eV, 0.5 μsec from 10^5 to 9×10^5 eV, and 0.2 μsec above 9×10^5 eV. At the lower neutron energies, the time channels were automatically increased by the analysis program to approximately $1/8$ the Doppler width (full width at $1/e$).¹⁵

An appropriate background, as determined from the blank foil, was subtracted from each signal. A correction was then made for the ^{239}Pu in the target by subtracting 0.6% of the ^{239}Pu fission cross section reported in Ref. 13, between 20 and 10^4 eV. The data in Ref. 13 do not extend below 20 eV; the cross section in Ref. 24 was therefore used from

17 to 20 eV. Above 10^4 eV, the ^{239}Pu correction was negligible. The corrections for the other isotopic contaminants in the sample were negligible. Typically, the larger ^{239}Pu resonances were roughly the same size as the smaller ^{238}Pu resonances. Imperfect ^{239}Pu subtraction, in part due to differing resolution functions, produced some of the apparently negative cross sections reported here, for instance at 66 and 75 eV.

The IASL-derived cross sections were produced by averaging the signals from the two detectors. Over the threshold region the fission fragment angular distribution would be expected to make this simple averaging invalid. However, angular distributions measured by other investigators^{4,8,25} indicate that the $55^\circ/80^\circ$ ratio would be ≤ 1.05 , so that the average would be changed by $\approx 2.5\%$ if such a correction were applied. Since the angular distributions are found to be well represented by the sum of Legendre polynomials P_0 and P_2 , the 55° signal (and hence the $55^\circ - 80^\circ$ average) can be taken as representative of the cross section integrated over all angles.

The AWRE-derived cross section was measured by a single 90° detector. Data from a 55° detector are being analyzed.

IV. ERRORS

In processing the data, the experimental uncertainties were separated into systematic (correlated) and random (uncorrelated) errors.¹⁵ Systematic errors included those that influence the level of the entire cross section, such as the uncertainty in the amount of

^{238}Pu exposed to the neutron beam. Random errors included those that varied with neutron flight time and/or signal level, such as the uncertainty in background subtraction, and those that varied from point to point, such as the statistical uncertainty in the number of fragments detected per time channel. Systematic errors (standard deviations) are listed in Table IV. By using $^{235}\text{U}(n,f)$ as a flux monitor and by averaging the ^{238}Pu signals, the overall systematic uncertainty was reduced to $\pm 5.3\%$.

An estimated uncertainty of $\pm 4\%$ in the ^{235}U reference cross section was included in the 5.3% systematic error, which then refers to the absolute value of the ^{238}Pu fission cross section rather than to a ratio to ^{235}U .

In averaging cross sections from different detectors or different recording modes, the error of the average was taken as the greater of the internal and external errors.

To ensure that neutron beam position and hence detector solid angles were as previously measured, careful optical alignment was made with cross hairs at each target position. The light of sight included the target cross hairs, cross hairs in the final beam collimator just below the sample chamber and in the initial beam collimator near ground level, and the center of the moderator just above the source. As a final check on beam position, fine gold cross hairs in the beam apertures at the top and bottom of the target chamber were exposed to the neutron beam. Postexperiment radioautographs of the gold showed that the neutron beam center was 0.04 ± 0.04 cm from the alignment axis.

The statistical uncertainty varied widely with the product of neutron flux and fission cross section. For instance, in the MeV region each 0.2- μ sec time channel contained several times 10^4 fragments. In contrast, the resonance at 18.6 eV, in a region of low flux, contained about 2000 observed fragments integrated over the resonance. The smaller resonance at 59.7 eV, in a region of higher flux, contained a total of about 500 observed fragments.

V. FISSION CROSS SECTION

A. Present measurement. Detailed pointwise tables of the ^{238}Pu fission cross section are available in Refs. 26 and 27. Integrals of the cross section for selected (approximately half-decade) energy intervals are listed in Table V, which also presents a comparison between the AWRE-derived²⁷ and LASL-derived²⁶ cross-section integrals. Figure 1 presents the LASL-derived cross section in graphical form. Reference 26 also includes a table of the fission cross section from 10^3 to 10^5 eV obtained from the drum camera (high resolution) recordings. These data show greater detail in the intermediate structure than Fig. 1.

Table VI lists the observed fission-resonance energies and areas below 500 eV, the region in which the number of levels missed is believed to be small. The uncertainty in the resonance energies is estimated to range from a few tenths of an eV at 20 eV neutron energy to one eV at 500 eV neutron energy.

Figure II illustrates the cumulative number of observed levels as a function of neutron energy below 500 eV. The straight line plotted is a least-squares fit to the 49 resonances reported here plus those at 3 and 10 eV reported in the ^{238}Pu total cross section¹¹ and in the ^{238}Pu fission cross section.^{1,2} These 51 resonances are assumed to belong to a population of $1/2^+$ levels, produced by the incidence of s-wave neutrons on the 0^+ target. The slope of the line, 0.106 levels/eV, corresponds to a mean level spacing of 9.5 eV, with a statistical uncertainty of ± 0.7 eV.²⁸ Additional uncertainties arise from the possible inclusion of small p-wave resonances in the sample and from possible missed levels, effects which tend to cancel each other.

Satisfactory agreement between the observed resonance spacing distribution and the Wigner spacing distribution is illustrated in Fig. III.

B. Comparison with other measurements. In the resonance region, comparison can be made with results of Stubbins et al.,¹ Gerasimov,² and Drake et al.¹⁰ Comparing well-resolved resonances measured by Stubbins et al. with our values for the same areas shows excellent agreement, much better than expected from the 40% normalization uncertainty quoted by them. For the three resonances below 100 eV observed by both Gerasimov and us, we obtain fission areas about twice as large as those of Gerasimov. The present IASL-derived results are $\sim 15\%$ higher than those of Drake et al.¹⁰ in the resonance region.

We observe a number of small resonances (five below 100 eV) previously unreported in either the accelerator fission or total cross sections. These were confirmed by the explosion-source experiment of Drake et al.,¹⁰ which had the advantages of a much purer ^{238}Pu sample and a stainless steel sample backing that eliminated the platinum resonances.

For fast neutrons, comparison can be made with Refs. 5, 6, and 8 in the region from 0.5 to 3.0 MeV. As illustrated in Fig. IV, the present results are in excellent agreement with those of Barton and Koontz,⁵ Ermagambetov and Smirenkin,⁶ and Fomushkin and Gutnikova.⁸ A discrepancy ($\sim 15\%$) between our values and those in Refs. 6 and 8 exists near 0.8 MeV. The earlier measurements by Butler and Sjoblom³ and Vorotnikov et al.⁴ in the plateau region between 1 and 3 MeV lie systematically about 20% higher than the four more recent determinations.

Comparison can also be made between the values reported here and the empirical relation σ_f (barns) = $-39.031 + 17.231 Z^2/A^{3/2}$, derived by Smith, Smith, and Henkel²⁹ from a fit to the first fission plateau between 2 and 5.5 MeV for thirteen isotopes ranging from radium to plutonium. Although ^{238}Pu lies slightly outside the range of the parameter $Z^2/A^{3/2}$ considered in the fit, agreement is excellent, with a value of 2.17 b predicted by the formula and an average experimental value of 2.2 ± 0.1 b between 2 and 3 MeV.

C. Intermediate structure. Intermediate structure has been observed in the subthreshold neutron-induced fission cross sections of a number of nuclides, notably ^{240}Pu , ^{237}Np , and ^{234}U . In ^{238}Pu this effect has been pointed out by Lynn³⁰ and by Young and Silbert,³¹ based on the present data.

The structure in question exhibits itself as a gross modulation of the fine structure resonances, with considerable enhancement at the intermediate structure peaks. It is attributed to the effects of coupling between the normal compound nuclear levels and the much less dense, high fissile levels in the second potential well of a double-peaked fission barrier.³² Lynn³⁰ and Weigmann³³ described the structure to be expected for various interaction conditions between the two potential wells.

Such structure is evident in Fig. 1. We have attempted to determine the mean spacing of the intermediate structure peaks both by (1) averaging the fission cross section over energy bins 10 to 100 times the average fine structure spacing of ~ 10 eV and (2) by a correlogram technique. The resulting value is 1200 ± 300 eV, a result similar to that obtained by simply counting the gross features of the fission cross section of Fig. 1.

In the region of resolved resonances in $^{238}\text{Pu}(n,f)$, the resonance at 285 eV exhibits an unusually large width and atypical shape. The resonances in the region of 285 eV have been fitted with a multilevel Breit-Wigner formula that yields a good fit to the 285-eV peak. The

derived width of the resonance is 3 to 4 eV; this is interpreted as being resonance width, greatly enhanced by the effect of intermediate structure. Individual resonance parameters, derived from a combination of fission and capture cross-section measurements, will be presented in a subsequent paper.

ACKNOWLEDGMENTS

Neutron cross sections derived from nuclear explosion neutron sources are the result of the joint efforts of many people. In particular, we wish to thank B. C. Diven and A. Hemmendinger (LASL) and R. Batchelor (AWRE), under whose supervision this work was done. We are indebted to the LASL Test Division for many contributions. At LASL, special thanks are due to J. G. Povelites for preparation of the ^{238}Pu sample, A. N. Ellis and E. R. Shunk for the experimental apparatus, P. A. Seeger for computer programming and data reduction, and J. D. Johnson for data reduction. At AWRE, we thank E. Moss for the preparation and installation of the recording equipment, A. H. F. Muggleton and C. Parsons for manufacture of the special surface barrier detectors, D. G. Piper and J. Pugh for experimental preparations, and K. Wyld for computer programming. We also wish to acknowledge the support furnished this project by O. D. Simpson, F. B. Simpson, J. F. Kunze, and R. M. Brugger of the Aerojet Nuclear Company, Idaho Falls, Idaho.

FOOTNOTES

- † Work supported under the auspices of the U.S. Atomic Energy Commission and the U.K. Atomic Energy Authority.
1. W. F. Stubbins, C. D. Bowman, G. F. Auchampaugh, and M. S. Coops, Phys. Rev. 154, 1111 (1967).
 2. V. F. Gerasimov, Sov. J. Nucl. Phys. 4, 706 (1967).
 3. D. K. Eutler and R. K. Sjoblom, Bull. Am. Phys. Soc. 8, 369 (1963).
 4. P. E. Vorotnikov, S. M. Dubrovina, G. A. Otroshchenko, and V. A. Shigin, Sov. J. Nucl. Phys. 3, 348 (1966).
 5. D. M. Barton and P. G. Koontz, Phys. Rev. 162, 1070 (1967).
 6. S. B. Ermagambetov and G. N. Smirenkin, Sov. At. Energy 25, 1364 (1968).
 7. S. B. Ermagambetov and G. N. Smirenkin, JETP Letters 9, 309 (1969).
 8. E. F. Fomushkin and E. K. Gutnikova, Sov. J. Nucl. Phys. 10, 529 (1970).
 9. M. G. Silbert, "Fission Cross Section of ^{238}Pu from Persimmon", Los Alamos Scientific Laboratory report LA-4108-MS (1969).
 10. D. M. Drake, C. D. Bowman, M. S. Coops, and R. W. Hoff, "Fission Cross Sections from Pommard", edited by P. A. Seeger, Los Alamos Scientific Laboratory report LA-4420, p. 101 (1970).
 11. T. E. Young, F. B. Simpson, J. R. Berreth, and M. S. Coops, Nucl. Sci. Eng. 30, 355 (1967).
 12. B. C. Diven, Report No. CONF-660925, 1966, p. 539; Ann. Rev. Nucl. Sci. 20, 79 (1970).

13. P-3 and W-8 Staff, "Fission Cross Sections from Petrel",
Los Alamos Scientific Laboratory report LA-3586 (1966).
14. A. Hemmendinger, B. C. Diven, W. K. Brown, A. Ellis, A. Furnish,
E. R. Shunk, and R. R. Fullwood, "Time-of-Flight Neutron Cross-Section
Measurements Made with Neutrons from Nuclear Explosions",
Los Alamos Scientific Laboratory report LA-3478, Part I (1967).
15. P. A. Seeger and D. W. Bergen, "Time-of-Flight Neutron Cross
Section Measurements Using Nuclear Explosions", Los Alamos Scientific
Laboratory report LA-3478, Part II (1966).
16. P. A. Seeger, A. Hemmendinger, and B. C. Diven, Nucl. Phys. A96,
605 (1957).
17. W. K. Brown, P. A. Seeger, and M. G. Silbert, "Neutron Flux Determination
in Time-of-Flight Cross-Section Measurements Using Underground Nuclear
Explosions", Los Alamos Scientific Laboratory report LA-4095 (1970).
18. W. K. Brown, A. N. Ellis, and D. D. Peterson, "A 90° ^3He Neutron
Spectrometer", Los Alamos Scientific Laboratory report LA-3752 (1967).
19. G. de Saussure, R. Gwin, L. W. Weston, R. W. Ingle, R. R. Fullwood,
and R. W. Hockenbury, Oak Ridge National Laboratory report ORNL-TM-1804
(1967).
20. W. G. Davey, Nucl. Sci. Eng. 26, 149 (1966); Nucl. Sci. Eng. 32,
35 (1968).
21. J. E. Simmons and R. L. Henkel, Phys. Rev. 120, 198 (1960).
22. J. H. Gibbons and R. L. Macklin, Phys. Rev. 153, 1356 (1967).

23. E. G. Bilpuch, K. K. Seth, C. D. Bowman, R. H. Tabony, R. C. Smith, and H. W. Newson, *Ann. Phys. (N.Y.)* 14, 387 (1961).
24. BNL-325, 2nd ed., Suppl. 2, "Neutron Cross Sections", edited by J. R. Stehn et al., Brookhaven National Laboratory (1965, 1966).
25. D. L. Shpak, D. N. Stepanov, and G. N. Smirenkin, *Sov. J. Nucl. Phys.* 9, 551 (1969).
26. M. G. Silbert, "Fission Cross Section of ^{238}Pu from Persimmon, Tabular Presentation", Los Alamos Scientific Laboratory report LA-4674-MS (1971).
27. A. Moat, "Fission Cross Section of ^{238}Pu from Persimmon", AWRE report O 13/72 (1972).
28. J. E. Lynn, "The Theory of Neutron Resonance Reactions" (Clarendon Press, Oxford, England, 1968), p. 103.
29. H. L. Smith, R. K. Smith, and R. L. Henkel, *Phys. Rev.* 125, 1329 (1962).
30. J. E. Lynn, "Physics and Chemistry of Fission, Proc. of the Second IAEA Symposium" (IAEA, Vienna, 1969), p. 249.
31. T. E. Young and M. G. Silbert, *Bull. Am. Phys. Soc.* 15, 648 (1970).
32. V. M. Strutinsky, *Nucl. Phys.* A95, 420 (1967).
33. H. Weigmann, *Z. Physik* 214, 7 (1968).

TABLE I. ^{235}U fission cross-section integrals; comparison between present experiment and Ref. 19.

E_1 (eV)	E_2 (eV)	$\int_{E_1}^{E_2} \sigma_f(E) dE$		$\frac{\text{Persimmon}}{\text{ORNL-RPI}}$
		Persimmon (b-eV)	ORNL-RPI ^a (b-eV)	
15.0	20.5	314	320	0.98
20.5	33.0	450	443	1.02
33	41	541	498	1.09
41	60	979	924	1.06
60	73	287	305	0.94
73	100	658	662	0.99
100	113	207	215	0.96
113	200	1890	1875	1.01
200	300	2030	2080	0.98
300	1000	7620	8100	0.94

^aRef. 19.

TABLE II. Reference ^{235}U fission cross section
above 10^4 eV.^a

E_n (eV)	$4\pi \frac{d\sigma_f}{d\Omega} (55^\circ)$ (b)	$4\pi \frac{d\sigma_f}{d\Omega} (90^\circ)$ (b)
1.05×10^4	3.10	3.10
2.03×10^4	2.58	2.58
3.03×10^4	2.28	2.28
4.09×10^4	2.08	2.08
4.99×10^4	1.96	1.96
6.10×10^4	1.85	1.85
7.45×10^4	1.74	1.74
9.10×10^4	1.65	1.65
1.01×10^5	1.63	1.63
1.50×10^5	1.50	1.50
2.02×10^5	1.41	1.41
3.02×10^5	1.29	1.29
4.08×10^5	1.22	1.22
4.50×10^5	1.19	1.19
4.98×10^5	1.17	1.17
5.50×10^5	1.15	1.14
6.08×10^5	1.14	1.13
6.72×10^5	1.13	1.11
7.43×10^5	1.15	1.13
8.21×10^5	1.18	1.15
9.07×10^5	1.21	1.16
1.00×10^6	1.22	1.17
1.11×10^6	1.22	1.17
1.22×10^6	1.22	1.17
1.35×10^6	1.22	1.17

Table II - continued

E_n (eV)	$4\pi \frac{d\sigma_f}{d\Omega} (55^\circ)$ (b)	$4\pi \frac{d\sigma_f}{d\Omega} (90^\circ)$ (b)
1.50×10^6	1.23	1.18
1.65×10^6	1.25	1.20
1.83×10^6	1.28	1.22
2.02×10^6	1.31	1.25
2.23×10^6	1.31	1.25
2.47×10^6	1.26	1.19
2.73×10^6	1.21	1.14
3.01×10^6	1.18	1.11

^aRefs. 20 and 21.

TABLE III. Comparison of experimental details, LASL and AWRE

Item	LASL	AWRE
Detectors	Diffused junction silicon, p-i-n, 125 μ thick, 1 μ window, 2000 Ω -cm resistivity	Surface barrier silicon, 500 μ thick, 0.1 μ window, 100 Ω -cm resistivity.
Amplifiers	Five decade, using logarithmic transistor.	Five decade, using two 2-1/2 decade logarithmic diodes.
Cabling	RG-219, approximately 1000 ft. between amplifier and recording equipment.	RG-219, approximately 75 ft. between amplifier and recording equipment.
Recording System	Oscilloscope-drum and streak camera systems, time resolution 0.2 μ sec and 1 μ sec.	Oscilloscope-disc camera system, overall time resolution 0.3 μ sec.

TABLE IV. Summary of systematic errors

A. ^{238}Pu signals	55° signal	80° signal
1. Target density	$\pm 3\%$	$\pm 3\%$
2. Detector solid angle	$\pm 3\%$	$\pm 2\%$
3. Fragment energy collected	$\pm 2\%$	$\pm 1\%$
4. Amplifier input resistance	$\pm 1\%$	$\pm 1\%$
B. Neutron flux		
1. Target density, ^{235}U	$\pm 2\%$	
2. ^{235}U fission cross section	$\pm 4\%$	

TABLE V. $^{238}\text{Pu}(n,f)$ cross-section integrals over wide neutron-energy ranges.

E_n (eV)	AWRE	LASL		
	$\int \sigma_f dE$ (b-eV)	$\int \sigma_f dE$ (b-eV)	$\int \sigma_f dE/E$ (b)	$\bar{\sigma}_f$ (b)
3×10^6	--	4.37×10^6	2.42	2.18
1×10^6	0.89×10^6	1.22×10^6	1.92	1.74
3×10^5	1.68×10^5	1.67×10^5	0.88	0.83
1×10^5	4.70×10^4	4.75×10^4	0.84	0.68
3×10^4	1.62×10^4	1.54×10^4	0.84	0.77
1×10^4	8.19×10^3	6.72×10^3	1.20	0.96
3×10^3	2.92×10^3	2.73×10^3	1.45	1.36
1×10^3	1.89×10^3	1.93×10^3	3.73	2.75
3×10^2	1.56×10^3	1.74×10^3	8.38	8.69
1×10^2	0.84×10^2	1.01×10^2	1.39	1.44

TABLE VI. Observed fission resonance energies and areas in the resolved-resonance region, 17 to 500 eV.

E_n (eV)	$\int \sigma_f dE$ (b-eV)	$\frac{\Gamma_n \Gamma_f}{\Gamma}$ (meV)	$\frac{\Gamma_n \Gamma_f}{\Gamma}$ (meV) / (eV) ^{1/2}
18.6	37.3 ± 15%	0.168	0.0390
32.2	1.1 ± 25%	0.0086	0.0015
36.6	0.4 ± 50%	0.0036	0.00059
59.8	1.7 ± 11%	0.025	0.0032
70.1	24.6 ± 10%	0.419	0.0500
77.7	0.3 ± 25%	0.0057	0.00064
83.0	62.4 ± 7%	1.257	0.1380
96.2	0.3 ± 50%	0.0070	0.0007
99.6	1.4 ± 20%	0.034	0.0034
110.1	19.7 ± 8%	0.526	0.0501
111.2	0.4 ± 50%	0.011	0.0010
113.6	46.8 ± 8%	1.290	0.1211
118.6	25.0 ± 8%	0.720	0.0661
122.4	119 ± 8%	3.54	0.320
129	0.2 ± 50%	0.0063	0.00055
132.4	3.5 ± 12%	0.113	0.0098
139.7	12.4 ± 9%	0.421	0.0356
151.1	102 ± 9%	3.74	0.304
165.0	1.3 ± 15%	0.052	0.0041
171.0	10.0 ± 9%	0.415	0.0317
176.8	33.5 ± 8%	1.438	0.1081
182.9	65.5 ± 8%	2.908	0.2150
192.5	240 ± 7%	11.21	0.808
203	5.3 ± 10%	0.261	0.0183
216	103 ± 8%	5.40	0.367

TABLE VI (continued)

E_n (eV)	$\int \sigma_f dE$ (b-eV)	$\frac{\Gamma_n \Gamma_f}{\Gamma}$ (meV)	$\frac{\Gamma_n \Gamma_f}{\Gamma}$ (meV)/(eV) ^{1/2}
221	14.0 \pm 10%	0.751	0.0505
232	0.3 \pm 25%	0.017	0.0011
245	43.1 \pm 8%	2.56	0.164
252	136 \pm 8%	8.32	0.524
261	0.7 \pm 30%	0.044	0.0027
285	372 \pm 10%	25.7	1.52
289	133 \pm 10%	9.33	0.549
300	406 \pm 7%	29.6	1.709
305	66.9 \pm 10%	4.95	0.283
320	58.0 \pm 7%	4.51	0.252
327	67.4 \pm 7%	5.35	0.296
337	27.5 \pm 8%	2.25	0.123
361	1.6 \pm 30%	0.14	0.0074
368	15.3 \pm 10%	1.37	0.071
382	1.4 \pm 35%	0.13	0.0066
391	7.8 \pm 15%	0.74	0.037
408	8.4 \pm 15%	0.83	0.041
419	131 \pm 8%	13.3	0.650
426	56.1 \pm 8%	5.80	0.281
448	38.4 \pm 10%	4.18	0.197
461	33.0 \pm 15%	3.69	0.172
465	40.4 \pm 15%	4.56	0.212
473	7.8 \pm 15%	0.90	0.041
496	10.6 \pm 15%	1.28	0.057

Fig. 1. Fission cross section of $^{238}\text{Pu} + n$, 18 eV to 3 MeV. Data of Table I of Ref. 26. Note that the top two plots have linear-logarithmic ordinates, linear below 1 b and logarithmic above 1 b; the third plot has a linear ordinate; the fourth plot has a logarithmic ordinate. Error bars refer only to the nonsystematic uncertainty (standard deviation). The systematic uncertainty is $\pm 5.3\%$.

$^{238}\text{Pu}(n,f)$

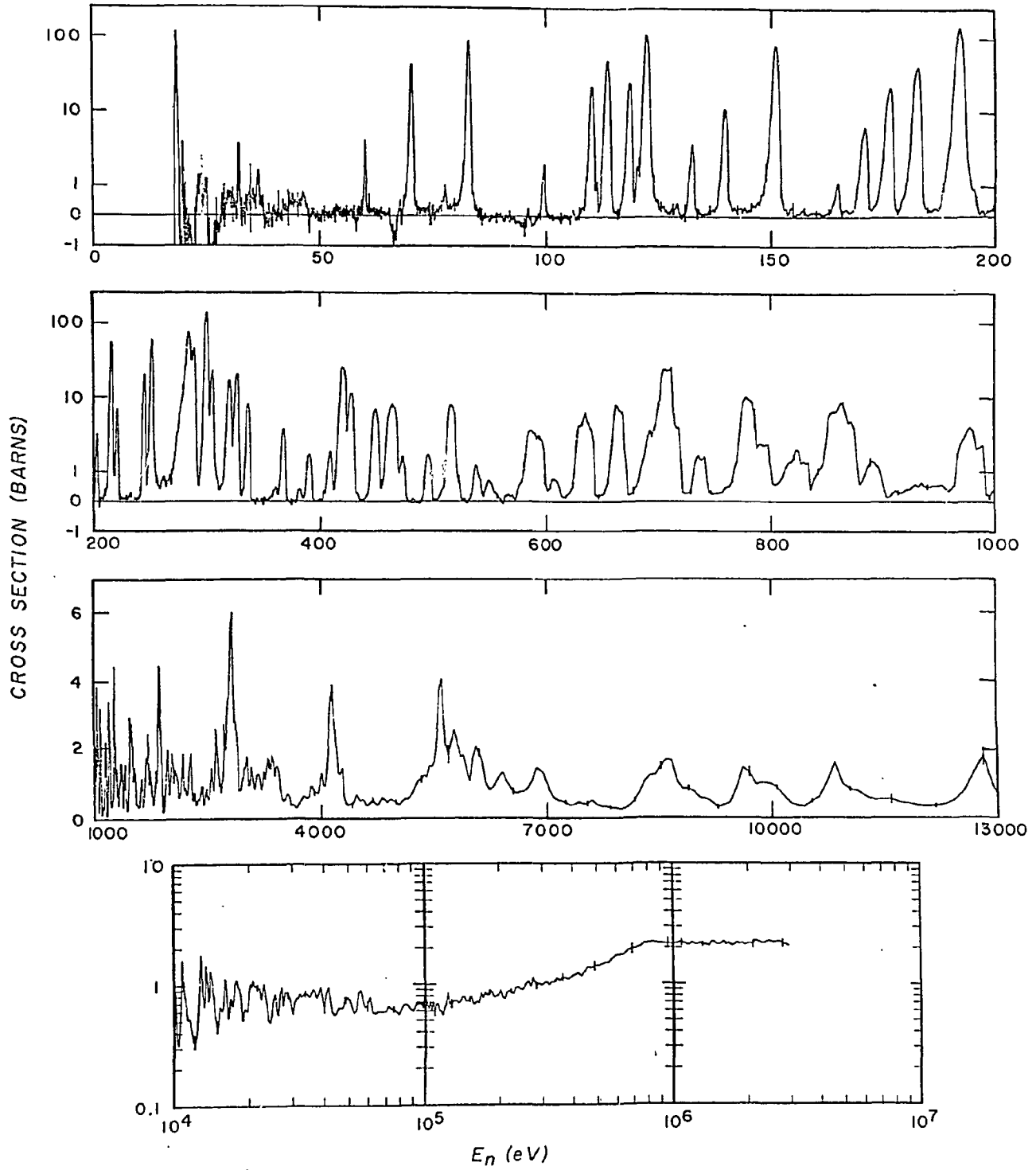


Figure 1

Fig. 2. Cumulative number of observed resonances vs. neutron energy. The solid straight line yielding the average level spacing is a least-squares fit to the points.

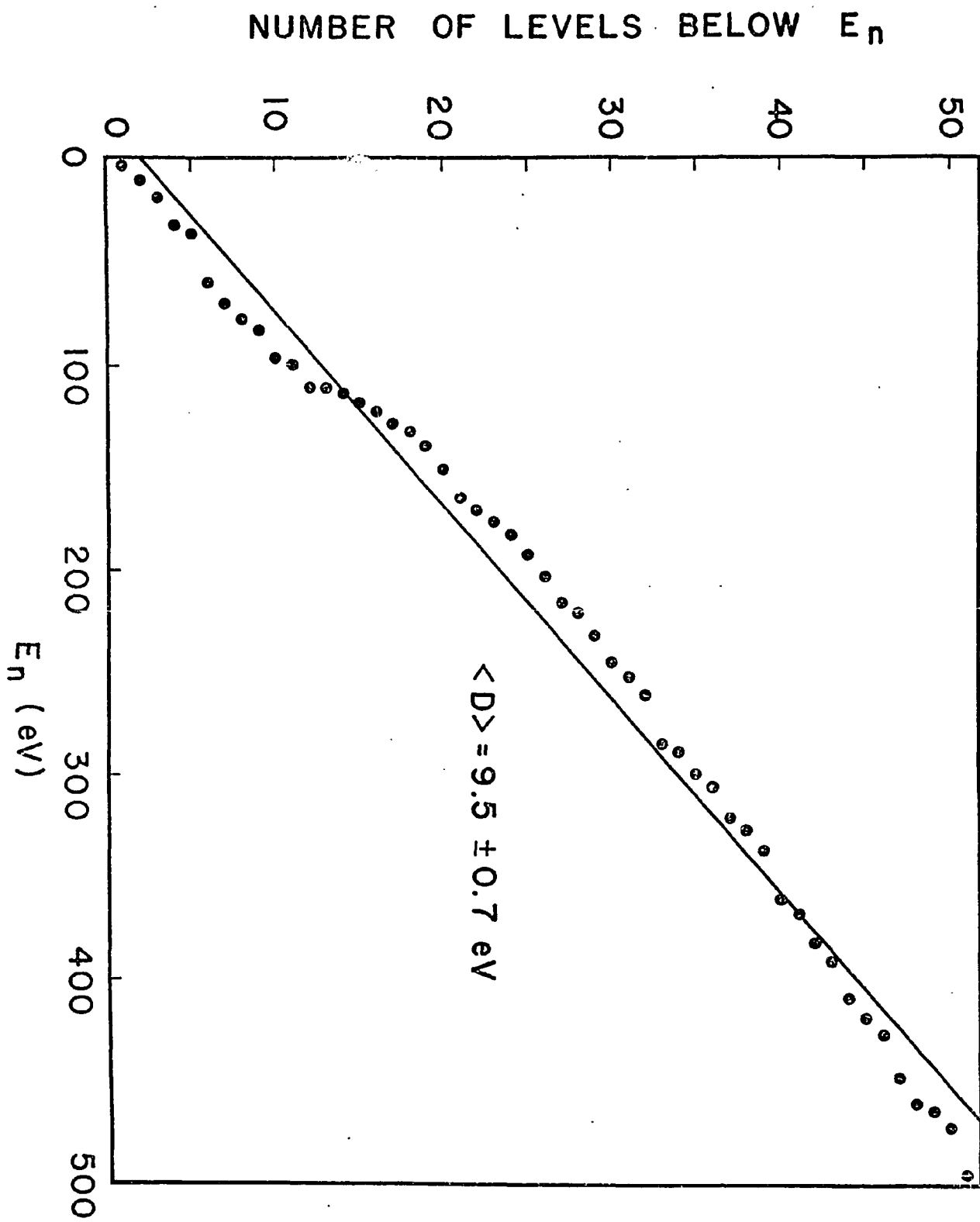


Figure 2

Fig. 3. Comparison of the observed level spacing distribution with the Wigner spacing distribution for 51 levels. The histogram is plotted at intervals of $\Delta X = 0.25$. The table compares intervals of $\Delta X = 0.50$. The values in the table yield chi-square of 1.25 with 3 degrees of freedom, a statistically acceptable fit.

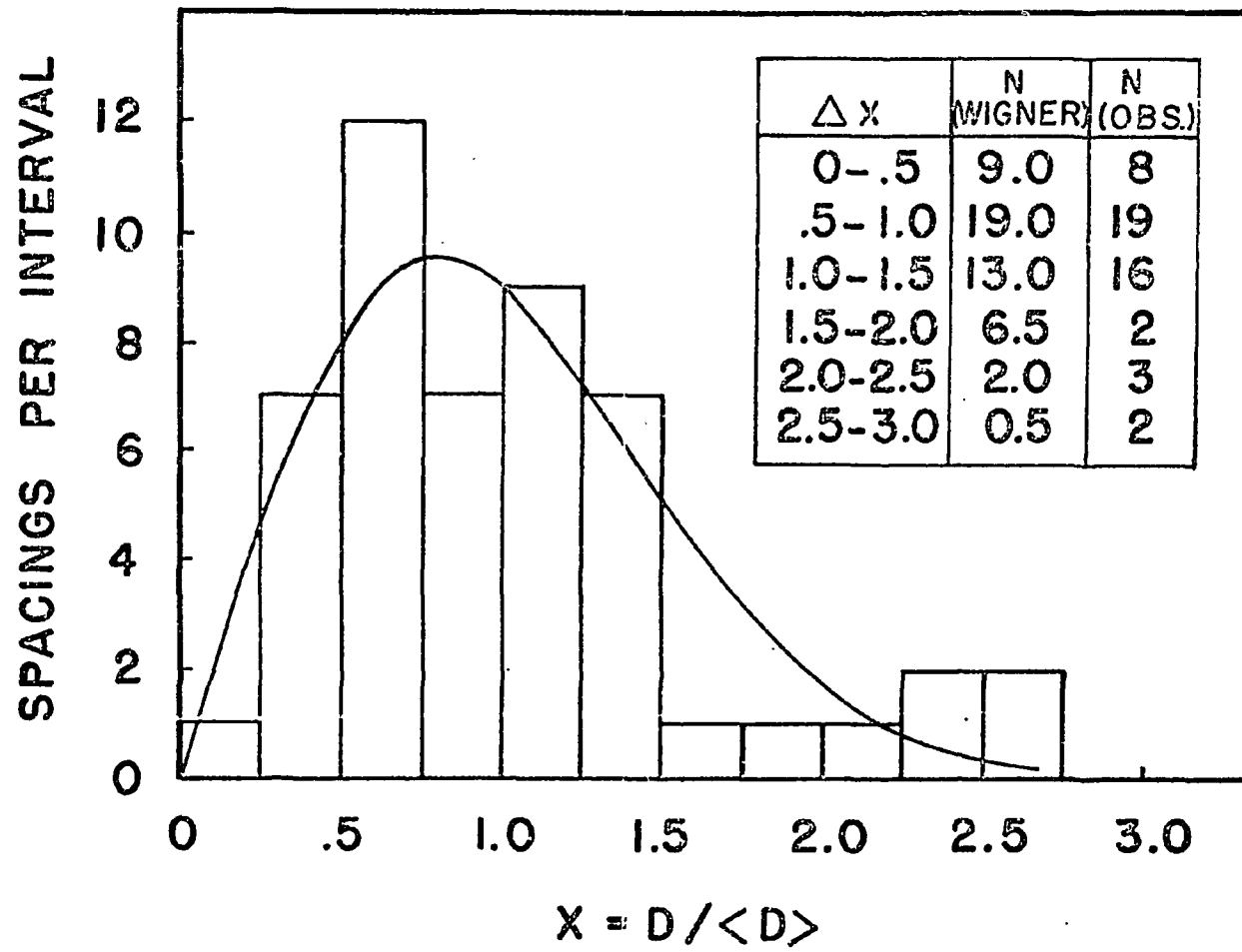


Figure 3

Fig. 4. Comparison of the cross section reported here with previous measurements in the neutron energy region 0.2 to 3.0 MeV. Representative uncertainties are indicated; these do not include the uncertainties in the reference cross sections used.

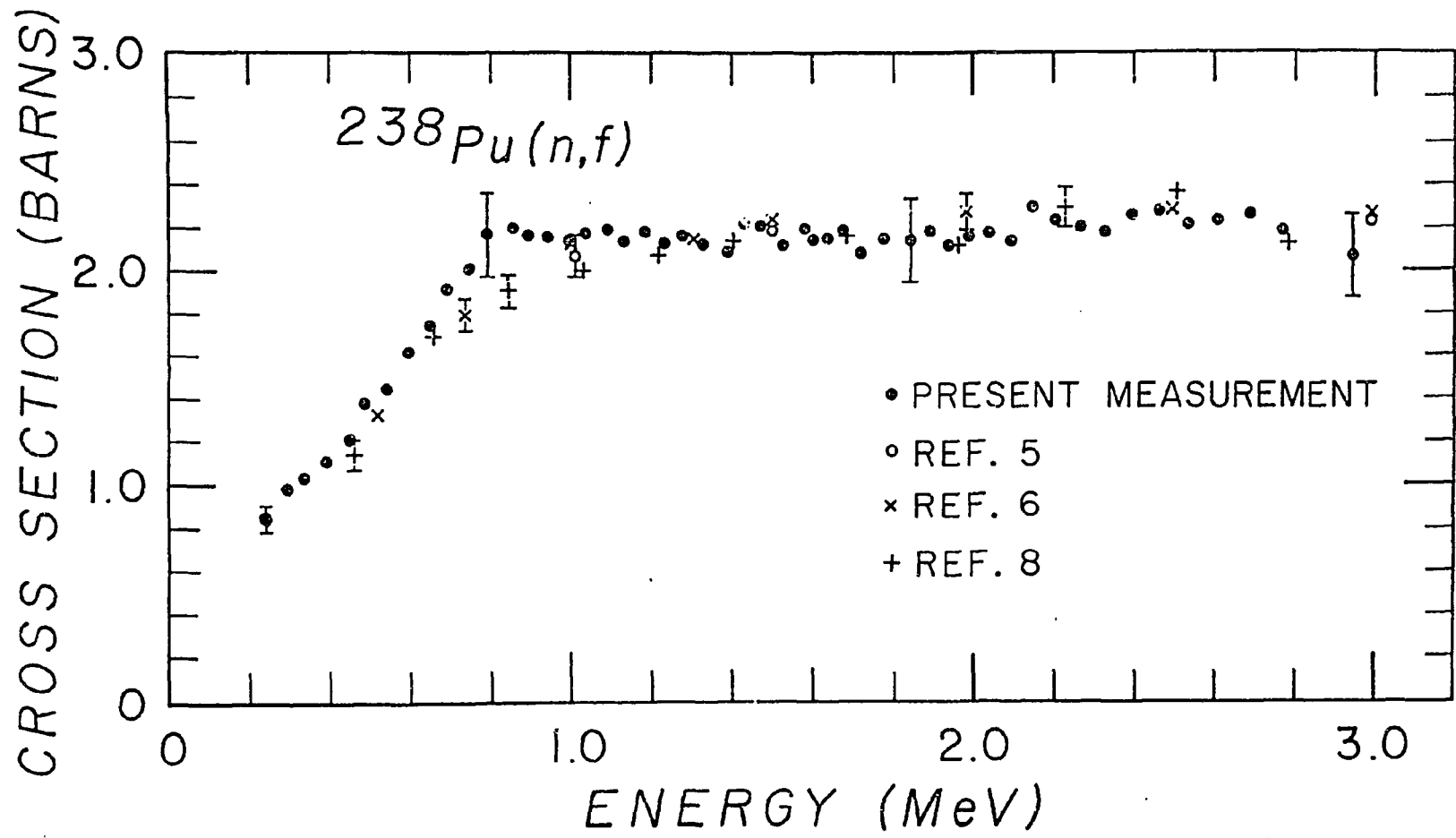


Figure 4